In silico and cell-based analyses reveal strong divergence between prediction and observation of T-cell–recognized tumor antigen T-cell epitopes

Received for publication, April 3, 2017, and in revised form, May 11, 2017 Published, Papers in Press, May 23, 2017, DOI 10.1074/jbc.M117.789511

Julien Schmidt[‡], Philippe Guillaume[‡], Danijel Dojcinovic[‡1], Julia Karbach[§], George Coukos[‡¶], and Immanuel Luescher[‡2]

From the [‡]Ludwig Institute for Cancer Research, University of Lausanne, 1066 Epalinges, Switzerland, the [§]Krankenhaus Nordwest, 60488 Frankfurt, Germany, and the [¶]Department of Oncology, University Hospital of Lausanne, 1011 Lausanne, Switzerland

Edited by Peter Cresswell

Tumor exomes provide comprehensive information on mutated, overexpressed genes and aberrant splicing, which can be exploited for personalized cancer immunotherapy. Of particular interest are mutated tumor antigen T-cell epitopes, because neoepitope-specific T cells often are tumoricidal. However, identifying tumor-specific T-cell epitopes is a major challenge. A widely used strategy relies on initial prediction of human leukocyte antigen-binding peptides by *in silico* algorithms, but the predictive power of this approach is unclear. Here, we used the human tumor antigen NY-ESO-1 (ESO) and the human leukocyte antigen variant HLA-A*0201 (A2) as a model and predicted *in silico* the 41 highest-affinity, A2-binding 8–11-mer peptides and assessed their binding, kinetic complex stability, and immunogenicity in A2-transgenic mice and on peripheral blood mononuclear cells from ESO-vaccinated melanoma patients. We found that 19 of the peptides strongly bound to A2, 10 of which formed stable A2-peptide complexes and induced $CD8^+$ T cells in A2-transgenic mice. However, only 5 of the peptides induced cognate T cells in humans; these peptides exhibited strong binding and complex stability and contained multiple large hydrophobic and aromatic amino acids. These results were not predicted by *in silico* algorithms and provide new clues to improving T-cell epitope identification. In conclusion, our findings indicate that only a small fraction of *in silico*–predicted A2-binding ESO peptides are immunogenic in humans, namely those that have high peptide-binding strength and complex stability. This observation highlights the need for improving *in silico* predictions of peptide immunogenicity.

Tumor exome and transcriptome sequences provide comprehensive information on mutated, overexpressed genes and aberrant splicing, which can be exploited for cancer immunotherapy. Of special interest are tumor antigen (TA)[3] T-cell epitopes containing mutation(s), because neoepitope-specific T cells often are tumoricidal (1, 2). To identify TA-derived T-cell epitopes, MHC-binding peptides are usually identified first. To this end MHC-peptide (pMHC) complexes can be isolated from tumor cells and their peptide cargo sequenced by mass spectrometry (3, 4). Alternatively *in silico* peptide predictions and peptide binding validation are used (5). Modern *in silico* peptide predictions involve machine-learning techniques like artificial neural networks (ANN) (6). A challenge in peptide prediction is the high diversity of human leukocyte antigen (HLA) alleles; even comprehensive databases, such as IEDB, contain no or limited data for rare alleles, which compromises training of prediction algorithms (7, 8). To improve prediction accuracy, pan prediction servers, like NetMHCpan or PickPocket, were introduced that exploit similarities between MHC alleles and their ligand-binding properties (9–11). Another difficulty is that MHC class I molecules present peptides of different lengths, usually 8–11 residues long. Gapped sequence alignments were introduced to improve predictions of peptides of different length (9, 12, 13). By including proteasomal cleavage predictions, peptide prediction accuracy can be further increased (8, 14). Different *in silico* MHC ligand prediction algorithms can be combined to reduce the number of peptide candidates (8, 15).

Only a small fraction of HLA ligands is immunogenic, and *in silico* prediction of these is challenging because of ambiguities of prediction parameters. According to some studies, immunogenicity correlates with peptide binding affinity (5), pMHC complex kinetic stability (16), or both (17). Moreover, it has been reported that immunogenic peptides contain large aliphatic and/or aromatic residues in TCR-accessible positions (18, 19). T-cell epitope prediction servers like NetTepi or IEDB immunogenicity integrate such parameters (18, 20). However, peptide immunogenicity also depends on other factors, such as the efficiency of their production and presentation by professional antigen-presenting cells (APCs) and on central tolerance (1, 2). For personalized cancer immunotherapy, it is crucial to

This work was supported by Swiss National Science Foundation Grant 310030_12533/1. The authors declare that they have no conflicts of interest with the contents of this article.

This article contains supplemental Tables S1 and S2 and Figs. S1–S4.

[1] Present address: Covance Central Laboratory Services Sárl, 1217 Meyrin, Switzerland.

[2] To whom correspondence should be addressed: 155 Chemin des Boveresses, 1066 Epalinges, Switzerland. Tel.: 41-21-692-5988; E-mail: immanuel.luescher@unil.ch.

[3] The abbreviations used are: TA, tumor antigen; HLA, human leukocyte antigen; A2, HLA-A*0201; ANN, artificial neural network; ESO, NY-ESO-1; CTL, cytotoxic T lymphocyte; PBMC, peripheral blood mononuclear cell; pMHC, peptide-MHC complex; TCR, T-cell receptor; IEDB, Immune Epitope Database; APC, antigen-presenting cell; DC, dendritic cell.

identify TA-specific T-cell epitopes, and the available procedures are error-prone (21).

To identify key parameters of $CD8^+$ T-cell epitopes, we used the cancer testis antigen NY-ESO-1 (ESO) and HLA-A*0201 (A2). This non-mutated TA is expressed on a wide range of tumors, is highly immunogenic, and has been used in diverse vaccine studies, and $CD8^+$ T-cell responses have been studied extensively (22–27). Four A2-restricted ESO epitopes have been described that are naturally produced and presented by APC, two of which are expressed by tumor cells (25, 28–31). ESO-specific $CD8^+$ T-cell responses in humans exhibit a strong immunodominance hierarchy and diverse HLA restrictions (32, 33). Here we used different *in silico* servers to predict the binding strength, complex kinetic stability, and immunogenicity of A2-restricted 8–11-mer ESO peptides. The 41 peptides with the highest predicted binding affinity were tested for (i) binding to A2 using a refolding, a peptide rebinding assay (34, 35), and an A2 stabilization assay on T2 cells (36); (ii) A2-peptide complex kinetic stability at 37 °C (34, 35, 37); (iii) peptide immunogenicity in A2/DR1 transgenic H-$2^{-/-}$ mice (36, 38–40); and (iv) recognition by $CD8^+$ T cells from ESO-vaccinated melanoma patients (29–31). Our results define parameters of peptide immunogenicity and provide new cues on how to improve T-cell epitope discovery.

Results

ESO peptide binding to A2

To predict the binding of ESO 8–11-mer peptides to A2, we used the NetMHC 3.4 server (5, 41–43). By setting an affinity threshold of 3000 nM, 41 peptides were obtained (Table 1). Of these, 19 were 10- or 11-mers, which was unusual, because normally the majority of A2 bound peptides are 9-mers (13). The immunodominant $ESO_{157-165}$ peptide had an IC_{50} of 1015 nM and would have been missed when using the recommended cutoff of 500 nM (28, 29). We also performed predictions using the IEDB MHC I prediction server (44) and obtained the same results plus 17 additional peptides with predicted IC_{50} values of 918–2700 nM, none of which have been reported previously (supplemental Table S1).

Binding of the peptides to A2 was measured in a refolding assay (45). The most efficient refolding was observed for peptide 4, referred to as 100%, followed by peptides 6 (90%), 5 (87%), 31 (83%), and 1 (80%) (Fig. 1, *A* and *B*). The correlation between measured and predicted peptide binding exhibited a Pearson coefficient of $r = 0.64$ and strong divergences for the peptides with high refolding scores (supplemental Fig. S1*A*). Similar correlations were observed when peptide binding was predicted with the more recent NetMHC 4.0 or NetMHCpan servers (9, 12) (supplemental Fig. S1, *B* and *C*). Comparable binding values were observed when using a peptide-rebinding assay ($r = 0.97$) (Fig. 1, *B* and *C*). Repeating these experiments with different batches of peptides cautions that errors in the peptides (*e.g.* impurities and degradations) can be larger than those of these assays. We also assessed ESO peptide binding by an A2 complex stabilization on $A2^+$, TAP^- T2 cells (36) and obtained grossly different results, which may be explained by the fact that A2 peptide stabilization on these cells relies on different mechanisms, the relative contributions of which are peptide-dependent (data not shown) (46).

Table 1
Peptides

No	Position[a]	Length	Sequence[a]	Affinity (nM)[b]	Stability (h)[c]	Epi score[d]	IEDB IS[e]
1	158-167	10	LLMWITQCFL	13	15.59	0.73	0.25
2	108-116	9	SLAQDAPPL	20	2.81	0.59	-0.06
3	86-94	9	RLLEFYLAM	23	4.21	0.63	0.22
4	159-167	9	LMWITQCFL	32	2.51	0.62	0.16
5	91-100	10	YLAMPFATPM	35	1.65	0.57	0.002
6	159-169	11	LMWITQCFLPV	35	7.15	0.68	0.17
7	161-169	9	WITQCFLPV	57	4.29	0.49	-0.06
8	108-118	11	SLAQDAPPLPV	69	4.45	0.59	-0.08
9	121-128	8	VLLKEFTV	112	5.53	0.63	0.02
10	126-135	10	FTVSGNILTI	172	0.97	0.42	0.01
11	86-96	11	RLLEFYLAMPF	192	2.08	0.42	0.08
12	120-128	9	GVLLKEFTV	194	0.78	0.44	-0.01
13	154-162	9	QQLSLLMWI	206	1.62	0.44	-0.21
14	110-118	9	AQDAPPLPV	229	0.54	0.37	0.009
15	91-98	8	YLAMPFAT	241	1.65	0.47	-0.03
16	157-167	11	SLLMWITQCFL	241	3.71	0.56	0.12
17	152-162	11	CLQQLSLLMWI	321	2.54	0.38	-0.36
18	86-93	8	RLLEFYLA	356	5.95	0.59	0.2
19	158-165	8	LLMWITQC	383	10.32	0.51	0.23
20	93-102	10	AMPFATPMEA	437	0.74	0.37	0.09
21	86-95	10	RLLEFYLAMP	442	0.61	0.42	0.13
22	148-156	9	SISSCLQQL	446	1.53	0.29	-0.45
23	145-153	9	LQLSISSCL	562	1.39	0.35	-0.37
24	122-132	11	LLKEFTVSGNI	760	0.81	0.37	0.09
25	157-166	10	SLLMWITQCF	771	1.19	0.29	0.07
26	162-171	10	ITQCFLPVFL	813	0.7	0.32	0.1
27	160-169	10	MWITQCFLPV	822	1.3	0.29	0.01
28	155-162	8	QLSLLMWI	831	1.49	0.39	-0.05
29	158-166	9	LLMWITQCF	949	4.22	0.38	0.2
30	162-169	8	ITQCFLPV	994	2.3	0.37	0.002
31	157-165	9	SLLMWITQC	1015	2.41	0.38	0.12
32	109-118	10	LAQDAPPLPV	1023	0.56	0.26	-0.01
33	132-140	9	ILTIRLTAA	1166	1.62	0.34	0.24
34	93-100	8	AMPFATPM	1706	0.81	0.28	0.18
35	152-160	9	CLQQLSLLM	1785	1.22	0.23	-0.34
36	146-156	11	QLSISSCLQQL	1814	0.97	0.29	-0.47
37	153-162	10	LQQLSLLMWI	1834	0.82	0.25	-0.25
38	71-80	10	GLNGCCRCGA	2380	0.98	0.28	-0.05
39	144-153	10	QLQLSISSCL	2404	0.91	0.25	-0.41
40	132-139	8	ILTIRLTA	2643	1.18	0.29	0.22
41	87-94	8	LLEFYLAM	2760	0.52	0.27	0.17

[a] MQAEGRGTGG STGDADGPGG PGIPDGPGGN AGGPGEAGAT GGRGPRGAGA ARASGPGGGA[60]
PRGPHGGAAS GLNGCCRCGA RGPESRLLEF YLAMPFATPM EAELARRSLA QDAPPLPVPG[120]
VLLKEFTVSG NILTIRLTAA DHRQLQLSIS SCLQQLSLLM WITQCFLPVF LAQPPSGQRR[180]

[b] Binding affinity (IC_{50}) predicted by NetMHC 3.4; cutoff 3000 nM

[c] Complex stability ($\tau_{1/2}$) predicted by NetMHCstabpan

[d] T-cell epitope score (AU) predicted by Netepi 1.0

[e] IEDB MHC I immunogenicity score (IS)

A2-ESO peptide complexes kinetic stability

The kinetic stability of the A2-ESO peptide complexes obtained in >30% yields was assessed at 37 °C, and their half-lives ($\tau_{1/2}$) were calculated (Fig. 2*A*). Of the 20 complexes analyzed, the $\tau_{1/2}$ ranged between 1.82 h (peptide 29) and 13.5 h (peptide 1). The most stable complexes were those containing the peptides 1, 4, 16, and 31 and the Flu $matrix_{58-66}$ peptide. These peptides also exhibited strong A2 binding (Fig. 1*A*); however, other peptides exhibited robust A2 binding, but low kinetic complex stability, and the overall correlation between measured A2 binding and complex kinetic stability was poor ($r = 0.54$) (Fig. 2*B*). The measured complex stabilities correlated even less well with those predicted by the NetMHCstabpan (9) or the NetMHCstab server (47) ($r = 0.31$ and 0.47) (supplemental Fig. S1, *D* and *E*). It noteworthy that the correlation between predicted complex stabilities and predicted binding affinities was better when using the NetMHC 3.4 rather than the more recent NetMHC 4.0 server ($r = 0.58$ and 0.33, respectively) (Fig. 2*C* and supplemental Fig. S1*F*).

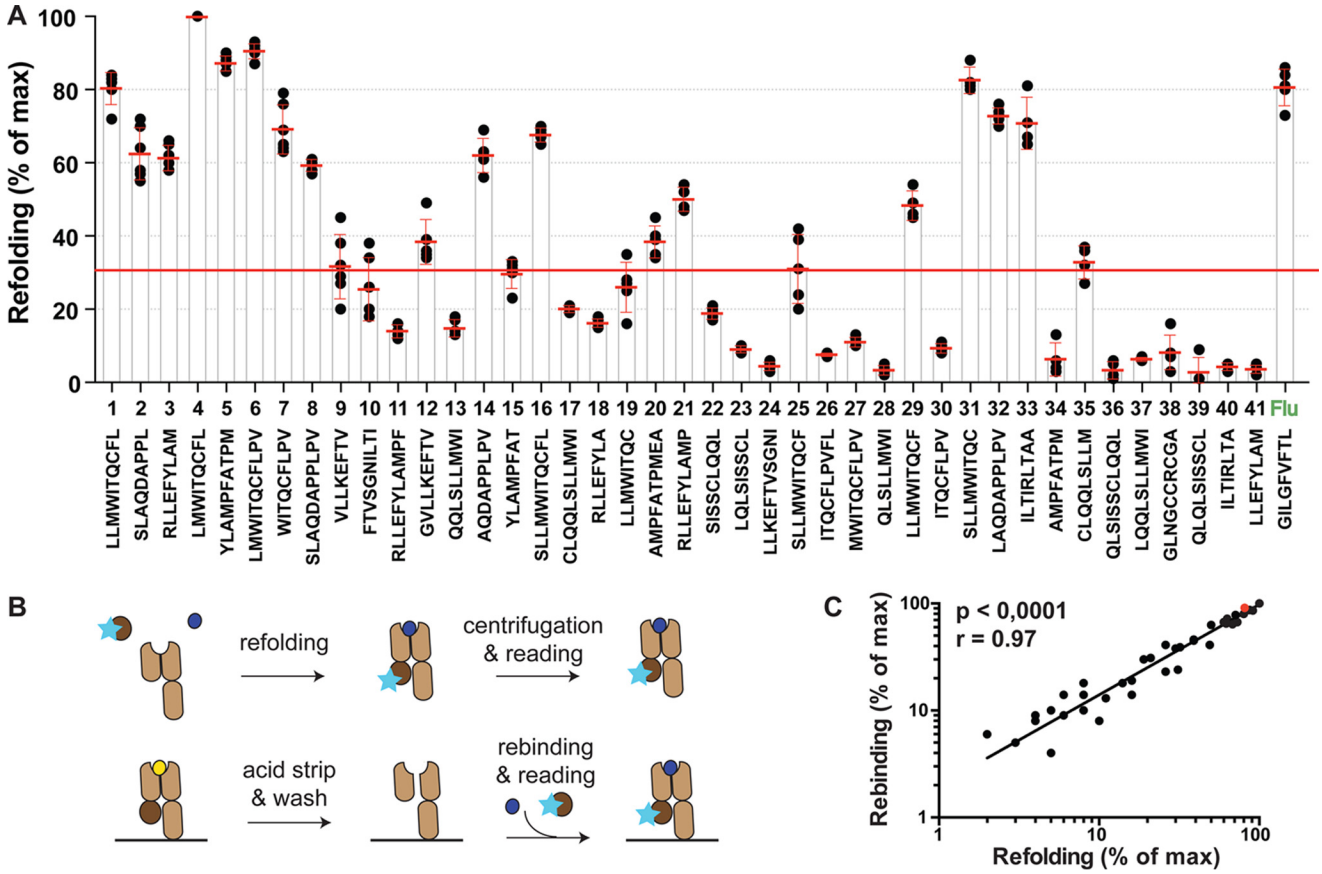

Figure 1. A2-ESO peptide binding. *A*, binding of ESO peptides to A2 was assessed by peptide-driven refolding assay. The *scatter blot* represents five independent experiments (*black dots*) and their mean values and S.D. (*red lines*). The *gray bars* represent the mean values. The Flu MP_{58-66} peptide served as positive control, and no peptide served as negative control. The *red line* indicates 30% refolding. *B*, depicted are the principles of the refolding (*top*) and rebinding (*bottom*) assays. The A2 heavy and light chains are shown in *light* and *dark brown*, respectively; the peptide is in *dark blue*, and Cy5 is in *light blue*. *C*, correlation between the results of the two assays; the inserted values indicate the Pearson coefficient *r* and the *p* value.

ESO peptide immunogenicity

To assess the ESO peptide immunogenicity in mice, groups of A2/DR1 transgenic H-$2^{-/-}$ animals were immunized with pools of five peptides of comparable A2 binding affinity. Fourteen days after a booster immunization, $CD8^+$ T-cell splenocytes were isolated and tested for IFNγ production by ELISPOT upon incubation with single peptide pulsed T2 cells. For the 10 peptides 1–4, 6, 8, 14, 16, 31, and 32, IFNγ responses were observed in the range of 30–108 spots/10^5 T cells (Fig. 3*A*). The strongest responses were observed for peptides 1, 4, 8, 16, and 32.

To assess peptide immunogenicity in humans, purified $CD8^+$ T cells from two melanoma patients vaccinated with recombinant vaccinia and fowl pox vectors expressing full-length ESO (23) were stimulated with the ESO peptides and assayed for IFNγ ELISPOT upon incubation with ESO peptide pulsed T2 cells. Strong IFNγ responses (600–800 spots/10^5 T cells) were observed on the cells from patient NW 1789 for peptides 1, 4, 6, 16, and 31 (Fig. 3*B* and supplemental Fig. S2*A*, *blue bars*). Lower responses were observed when autologous DC were used as APC (Fig. 3*B* and supplemental Fig. S2*A*, *red bars*). The peptide-dependent variations of the reductions may be explained by biased peptide presentation by T2 cells; *e.g.* the peptides 6 and 31 had higher binding scores on T cells than the peptides 1, 4, and 16. It may also be that on DC some peptides are presented by HLA alleles other than A2, which on T2 cells is unlikely, because they express A2 and only scant levels of HLA-B51 and Cw1 (supplemental Fig. S2*B*) (48). For the peptides 4, 16, and 31 $CD8^+$ T-cell responses have been described previously (supplemental Fig. S3). The peptide $ESO_{155-163}$ was missed, because its predicted binding affinity was 3319 nM, *i.e.* above the cutoff of 3000 nM used. The A2-restriced $CD8^+$ T-cell responses for peptides 1 and 6 have not been reported previously. Remarkably, ESO peptides 2, 3, 8, and 14 were immunogenic in A2 transgenic mice, but not in humans (Fig. 3).

Parameters defining ESO peptide immunogenicity

The peptides that were immunogenic in humans exhibited the highest A2 binding and kinetic complex stability (Fig. 2*B*). For the peptides immunogenic in mice only, both parameters were slightly lower. All immunogenic peptides exhibited complex stabilities of >4 h and refolding scores of >50%, and all non-immunogenic peptides exhibited lower values. No such correlation was observed when peptide-binding affinity was predicted using the NetMHC 3.4 (6, 42), NetMHC 4.0 (12), or NetMHCpan (9) server or kinetic A2-ESO peptide complex stability using the NetMHCstab (47) or NetMHCstabpan (16) server (Fig. 2*C* and supplemental Fig. S1). However, for most of the ESO peptides, the T-cell epitope scores predicted by the NetTepi server (20) correlated better with the measured bind-

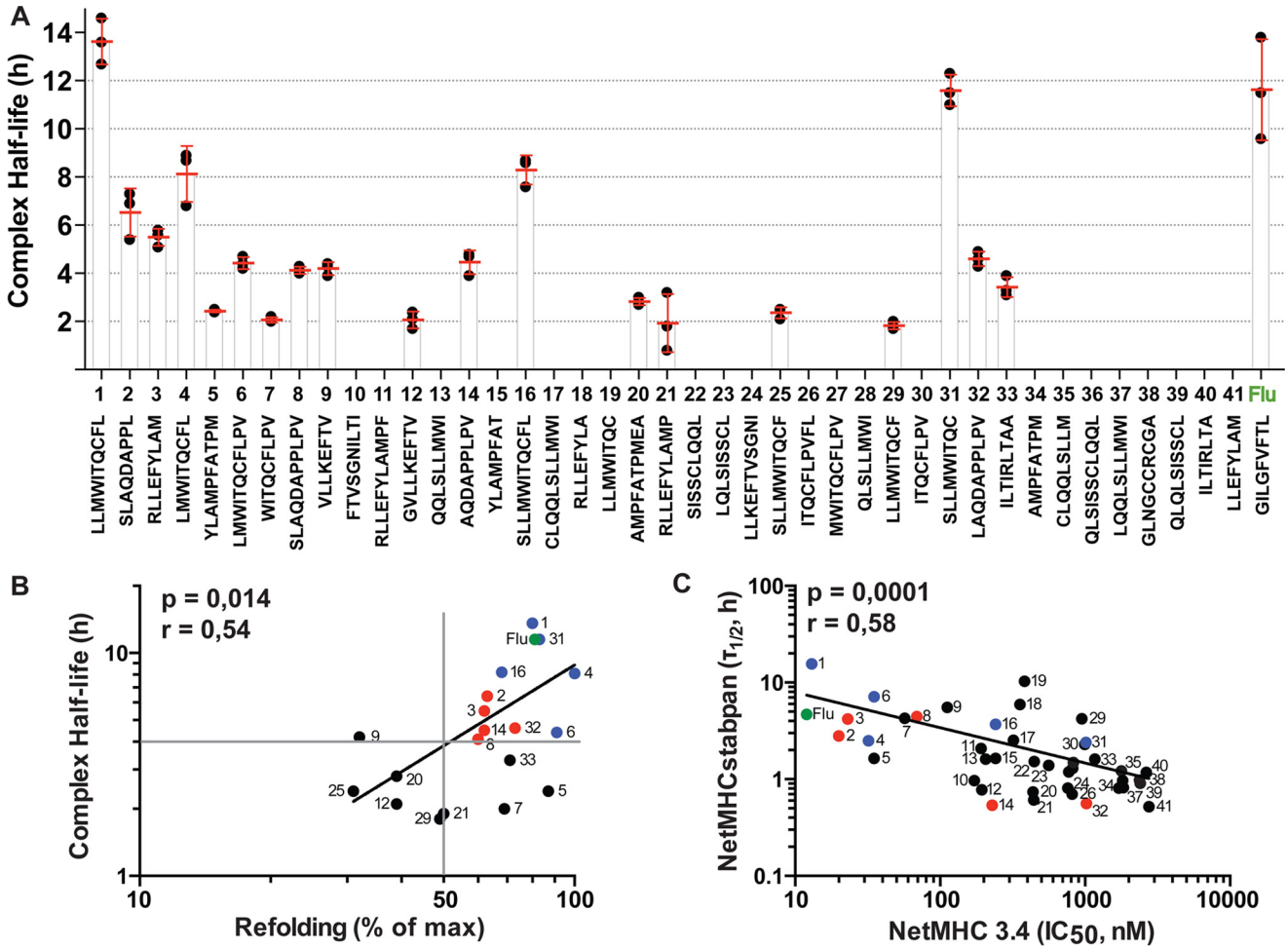

Figure 2. A2-ESO peptide complex kinetic stability. *A*, the A2-ESO peptide complexes for which refolding efficiency was >30% were incubated at 37 °C for different period of times, and the complex content was assessed. Half-lives were calculated and are represented in hours. The *scatter blot* represents three independent experiments (*black dots*) and their mean values and S.D. (*red lines*). The *gray bars* represent the mean values. *B*, correlation between measured kinetic complex stability ($\tau_{1/2}$ in h) and refolding score (% of max). The *numbers* designate the peptides, *Flu* indicates the influenza MP_{58-66} peptide (*green*), *p* is the *p* value, and *r* is the Pearson coefficient. *Dots* in *blue* represent peptides immunogenic in humans and mice, *red dots* represent those immunogenic only in A2 transgenic mice, and *black dots* represent non-immunogenic peptides. *C*, correlation between the NetMHC 3.4 predicted ESO peptides binding affinities (IC_{50} in nM) and NetMHCstabpan predicted complex stabilities ($\tau_{1/2}$ in h). The inserted *numbers* and the color coding are as in *B*.

ing strength and kinetic complex stability, respectively (Fig. 4, *A* and *B*). The three outliers included the therapeutically important peptide 31.

Of the ten ESO immunogenic peptides, five (peptides 1, 4, 6, 16, and 31) contained the $ESO_{159-165}$ sequence (LMWITQC) and were immunogenic in humans and A2 transgenic mice (Fig. 4, *C* and *E*). Peptides 2, 8, 14, and 32 were immunogenic only in mice and contained the sequence $ESO_{110-116}$ (AQDAPPL). Only the sequence of the ESO_{86-94} peptide was outside these two registers (Figs. 3 and 4, *C* and *E*). When bound to A2, generally the side chains of the second and the last (C-terminal) residues occupy the B and F pockets, whereas the side chains of the others are solvent-exposed to different degrees, and some can be secondary anchor residues (49–51). The peptides comprising the $ESO_{159-165}$ core sequence exhibited four or five large aliphatic and/or aromatic residues in these positions, whereas the peptides containing the $ESO_{110-116}$ core sequence only one or none (Fig. 4*D*). Two studies have shown that immunogenic peptides express such amino acids in solvent-exposed positions (18, 19). Indeed, the immunogenicity scores calculated with the IEDB immunogenicity predictor (http://tools.iedb.org/immunogenicity/),[4] which takes TCR propensity into account, were higher for the peptides containing the $ESO_{159-165}$ core sequence (0.17–0.25) than those containing the $ESO_{110-116}$ sequence (−0.06–0.009) (Table 1).

The correlations between predicted and measured peptide binding and kinetic pMHC complex stability in our study were poorer compared with those reported in other studies (supplemental Fig. S1, *A–E*) (9, 16, 42, 43). In these studies and for the training of the prediction servers, pathogen-derived antigens were used. To address the question of whether there are differences between TA and pathogen-derived peptides, we examined 149 non-mutated TA and 129 viral T-cell epitopes. All peptides were A2-restricted nonamers and collected from databases (supplemental Table S2). Positional amino acid usage of these peptides was analyzed with the Seq2Logo server (52). This revealed that in the main A2 anchor positions, 2 and 9, Leu was

[4] Please note that the JBC is not responsible for the long-term archiving and maintenance of this site or any other third party hosted site.

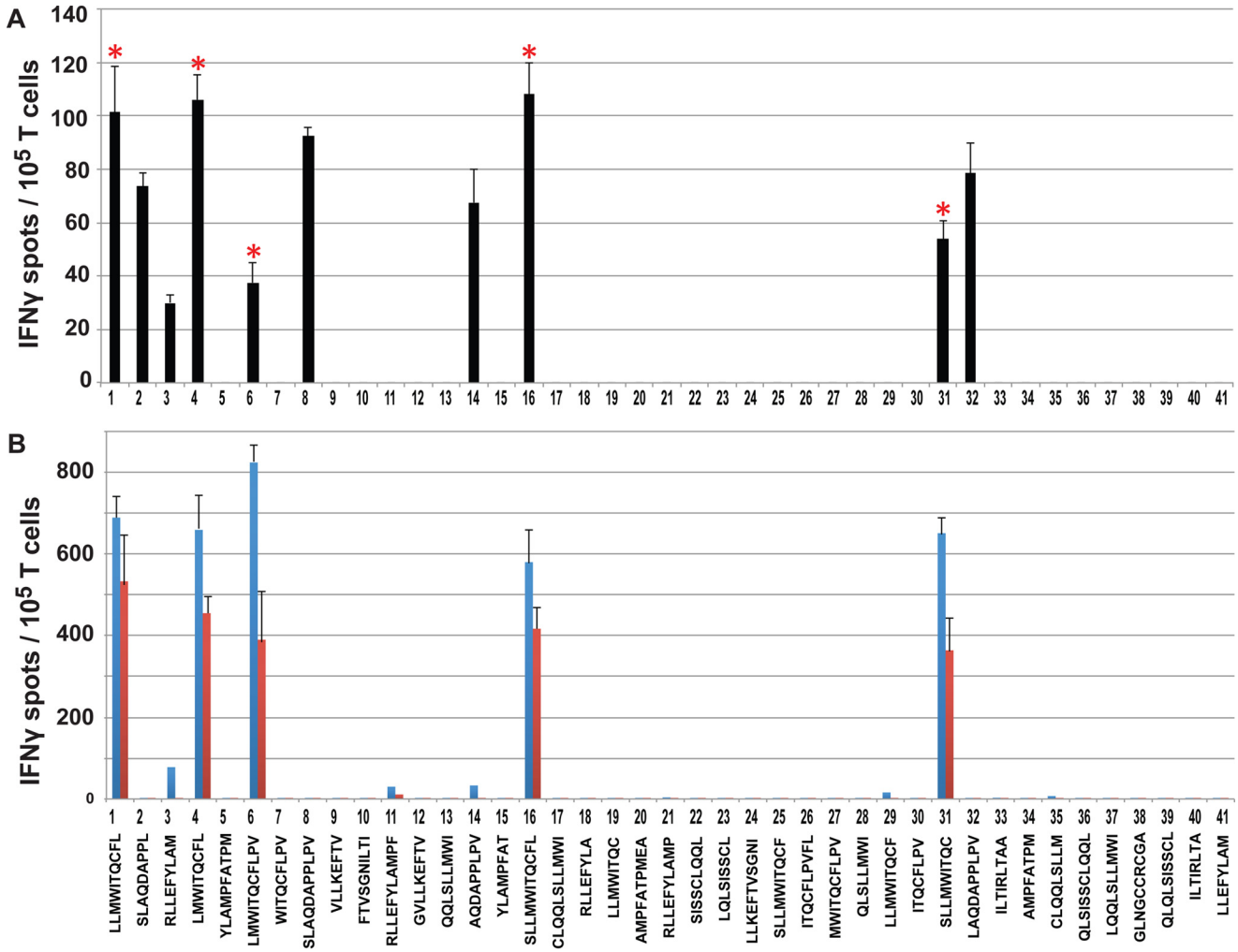

Figure 3. Immunogenicity of ESO peptides. *A*, groups of A2 transgenic, H-2$^{-/-}$ mice ($n = 5$) were immunized with peptide pools in incomplete Freund's adjuvant (IFA) and CpG. After one booster immunization, CD8$^+$ splenocytes were isolated and assayed for IFNγ production by ELISPOT upon stimulation with T2 cells pulsed with 1 μM of peptide. Nonspecific values measured in the absence of peptide were subtracted. Mean values and S.D. were calculated from two experiments. The *red asterisks* indicate peptides immunogenic in mice and humans. *B*, PBMC from ESO vaccinated patients NW 1789 and NW 3276 were stimulated once with the indicated peptide and IFNγ responses assessed by ELISPOT upon stimulation with peptide pulsed T2 cells (*blue bars*) or autologous DC (*red bars*). Nonspecific responses observed in the absence of peptide were subtracted. Mean values and S.D. were calculated from two experiments.

more frequent in TA peptides, especially in P9, in which Val was the most abundant residue in viral peptides (supplemental Fig. S4, *A* and *B*). Moreover, viral peptides exhibited higher amino acid diversity especially in positions 3 and 7, which typically are secondary A2 anchor residues (50, 51). We next calculated the average hydrophobicity scores for the residues in positions 1–9 for the two sets of peptides using the scales published by Kyte and Doolittle (53). The hydrophobicity was highest for the residues in position 2 and 9 and lowest for those in position 4 (supplemental Fig. S4*C*). Similar results were obtained when other amino acid hydrophobicity scales were used, *i.e.* those determined by Hopp and Woods (70), Abraham and Leo (71), Black and Mould (72), Sweet and Eisenberg (73), and Roseman (74), as detailed in http://web.expasy.org/protscale/ (supplemental Fig. S4*D*). The TA peptides exhibited higher hydrophobicity in all positions, except for position 3. In position 4 viral but not TA peptide frequently contained acidic residues, resulting in greatly reduced average hydrophobicity. As illustrated in structure of the A2-HIV RT$_{309-317}$ complex, an acidic residue in position 4 can stably bind to the A2 α1 helix (Arg-65) (51). Moreover, viral peptides contained more polar and/or charged residues in positions 1 and 7 than TA peptides, accounting for their overall modestly reduced hydrophobicity. Collectively these results argue that at large there exist differences between TA and viral peptides, notably in amino acid usages in A2 anchor positions.

Discussion

A widely used strategy to identify T-cell epitopes consists of first predicting HLA binding peptides by *in silico* algorithms (13, 34, 35, 54). Here we predicted A2-restricted 8–11-mer peptides of ESO using the NetMHC 3.4 and IEDB servers and obtained partially overlapping results, which was explained by that these servers are based on related ANN (Table 1 and supplemental Table S1) (6, 41, 42, 44). Testing of the 41 peptides with the highest predicted binding affinity gave very similar results when using the refolding or peptide rebinding assay (Fig. 1).

There exist diverse *in silico* MHC-peptide binding predictors of which the ANN based NetMHC servers performed best in

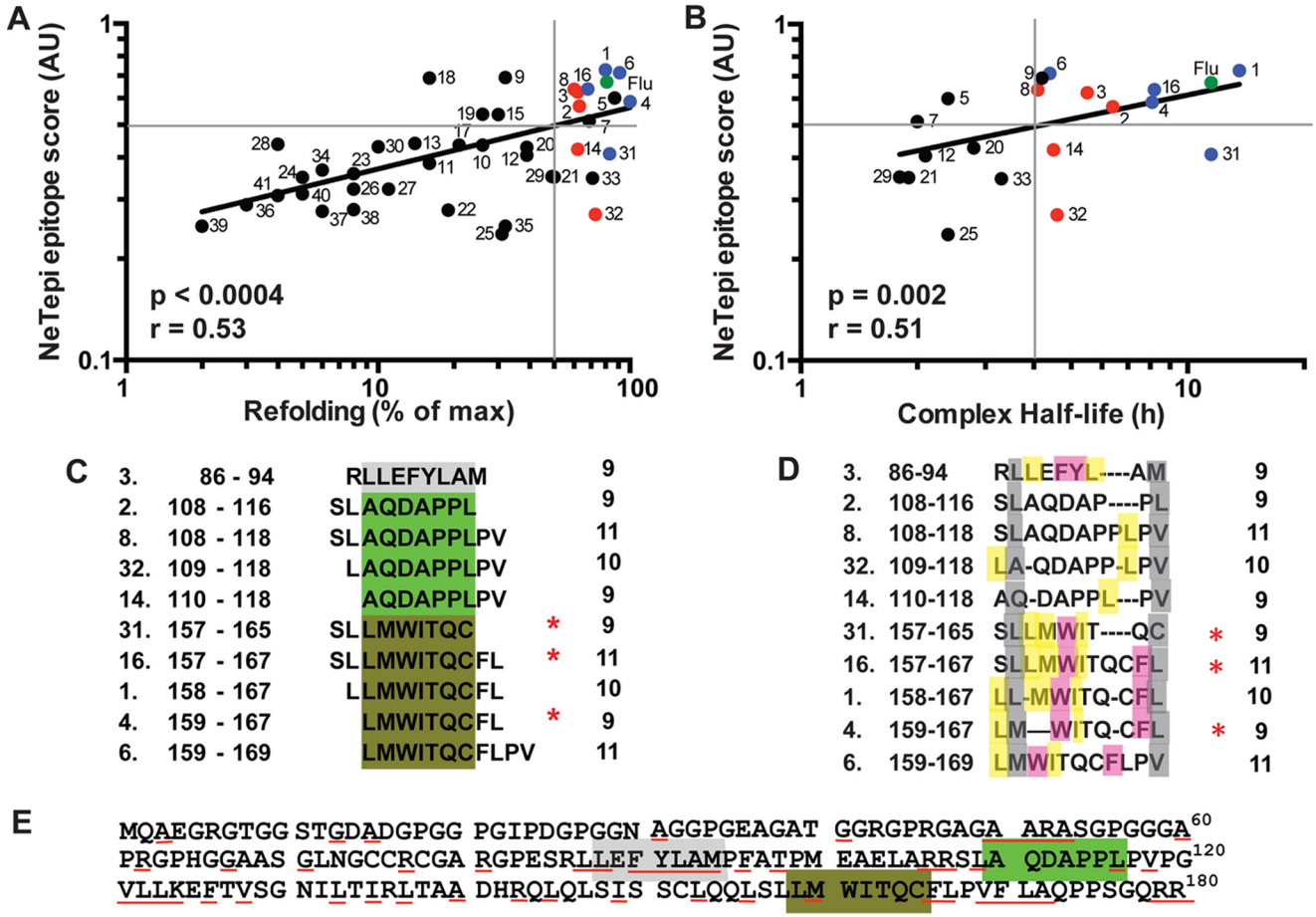

Figure 4. Immunogenicity of ESO peptides. *A* and *B*, correlations between the measured refolding (*x* axis; in %) (*A*) or A2-ESO-peptide complex kinetic stability (*x* axis $\tau_{1/2}$ in h) (*B*) and the epitope score predicted by the NetTepi server (*y* axis; in AU). The inserted *vertical lines* mark the 50% refolding score (*A*) or $\tau_{1/2}$ of 4 h, and the *horizontal line* represents the NetTepi score of 0.5 AU. The *numbers* designate the peptides, *Flu* indicates the influenza MP_{58-66} peptide (*green*), *p* is the *p* value, and *r* is the Pearson coefficient. *Blue dots* represent peptides immunogenic in humans and in mice, *red dots* represent those immunogenic only in A2 transgenic mice, and *black dots* represent non-immunogenic peptides. *C*, the immunogenic peptides containing the $ESO_{159-165}$ sequence are highlighted in *olive green*, those containing the $ESO_{110-116}$ sequence are in *light green*, and the one containing the ESO_{87-93} sequence is in *gray*. The *numbers* at *left* indicate the peptide number, those at *right* indicate the peptide length, and the *red stars* mark previously reported immunogenic peptides. *D*, the immunogenic peptides are represented with the potentially solvent-exposed amino acids in *bold*; highlighted in *yellow* are large hydrophobic residues, in *magenta* are the aromatic residues, and in *gray* are the main A2 anchor residues. *E*, the ESO sequence with the three immunogenic core sequences highlighted as in *C*. The residues shown in *underlined red* indicate proteasomal cleavage sites as predicted by the NetChop 3.1 server.

benchmark studies (8, 43, 55). We examined correlations between measured A2 ESO peptide binding and NetMHC 3.4 and the more recent NetMHC 4.0 or NetMHCpan 3.0 servers that allow insertions and deletions in peptide alignments and integration of multiple receptor and peptide length data sets, respectively (6, 9, 12, 42). Surprisingly, these refinements did not improve the correlations between measured and predicted ESO-peptide binding (supplemental Fig. S1, *A–C*). Poorer correlations were observed when peptide binding was predicted with the PickPocket, SYFPEITHI, or Rankpeptide servers, which is consistent with other reports (8, 11, 43, 55).[5] One explanation for the modest correlation between measured and predicted ESO peptide binding could be that the predicted binding affinities represent IC_{50} values in nM, whereas in our study relative binding values were measured at a fixed peptide concentration. However, in our system the measured IC_{50} values correlated even less well with NetMHC 3.4 predicted values ($r = 0.56$, $p < 0.0001$).[5]

We next measured the A2-ESO complex stabilities and found that the measured values poorly correlated with those predicted by the NetMHCstab and the more recent NetMHCstabpan server (supplemental Fig. S1, *D* and *E*) (16, 47). The measured ESO peptide binding and kinetic complex stability exhibited a modest correlation (Fig. 2*B*), which is consistent with the fact that peptide binding and kinetic pMHC complex stability can diverge; it has been shown that for complex stability, but much less for peptide binding affinity, fitting of the side chains of the residues in position 2 and 3 into HLA binding pockets is critical (37, 47, 56). In this plot all immunogenic peptides exhibited complex stabilities of >4 h and peptide binding efficiencies of >50% (Figs. 2*B* and 3 and Table 1). The highest peptide-binding strengths and complex stabilities were observed for the ESO peptides immunogenic in humans, followed by those immunogenic in A2 transgenic mice only. Our results are in accordance with an analysis of large data sets

[5] J. Schmidt, P. Guillaume, D. Dojcinovic, J. Karbach, G. Coukos, and I. Luescher, unpublished results.

showing that immunogenic peptides typically exhibit high binding affinity and high complex kinetic stability (57) but are at variance with studies reporting that peptide immunogenicity correlates with binding affinity (5, 34, 58) and pMHC complex kinetic stability (16, 34, 37), respectively. No significant correlation was observed between peptide immunogenicity, binding strength, and complex kinetic stability when complex stability was predicted by the NetMHCstabpan and binding affinity by the NetMHC 3.4 or NetMHC 4.0 server (Figs. 2*C* and 3 and supplemental Fig. S1*F*). There was also no correlation between peptide immunogenicity and predicted binding affinity and kinetic complex stability, respectively (Fig. 3 and supplemental Fig. S1, *A–E*, and Table 1). Moreover, our results caution that selection of peptides based *in silico* predictions using a cutoff affinity of 500 nM is prone to miss immunogenic peptides: in our study three peptides, including the clinically important peptide 31 (supplemental Fig. S3 and Table 1). The same is true for other clinically important TA epitopes like the A2-restricted Melan-A_{26-35} (EAAGIGILTV) (5164 nM), survivin$_{96-104}$ (LTLGEFLKL) (2002 nM), or CEA$_{694-702}$ (GVLVGVALI) (833 nM) peptides (http://www.iedb.org).[4] It is important to note that CTL tumor control depends more on the affinity of pMHC-TCR than on MHC-peptide binding (59).

The correlations between measured and predicted peptide-binding strength and kinetic complex stability were poorer in our study compared with those in other studies (supplemental Fig. S1, *A–E*) (9, 16, 42, 43). In these and for training of the prediction servers, pathogen-derived antigens were mainly used. Tumor antigens excluding neoantigens are *a priori* self-antigens and hence are subject to central tolerance, which is not the case for pathogen-derived antigens (60, 61). By comparing 149 TA and 129 viral A2 restricted nona-peptides, we observed significant differences in amino acid usages and average hydrophobicity in the potential secondary anchor residues in positions 1, 4, and 7 and smaller ones in the potential main A2 anchor residues in positions 2 and 9 (supplemental Table S2 and Fig. S4). It has been demonstrated that changes in HLA-peptide anchoring can alter the conformation and flexibility of pMHC complexes and thus their interaction with TCR (62–65). The significance of such changes is illustrated, for example, by modification of a potential main anchor residue (A27L) in the Melan-A_{26-25} peptide, which resulted in different TCR interactions and different outcomes of vaccine trials (64, 65). Thus the limited *in silico* prediction accuracy of TA peptides may be explained by that the servers were trained on pathogen-derived peptides. It is noteworthy that a substantial fraction of neoepitopes contains a mutation in an MHC anchor position, some of which may affect T-cell recognition via structural changes in the pMHC complex and binding to TCR (1, 2, 15, 58, 62, 63). It should be mentioned that most neoepitopes contain a stochastic somatic mutation, which can have different and diverse effects, making general predictions difficult.

An unexpected finding was that immunization of A2 transgenic mice induced CTLs for 10 of the ESO peptides, whereas in humans T cells specific for only five were observed (Figs. 3 and supplemental Figs. S2 and S3). This observation cautions that peptides can be immunogenic in HLA transgenic mice but not in humans. All ESO peptides that were immunogenic in humans contained the sequence ESO$_{159-165}$ (LMWITQC) (Figs. 3 and 4, *C–E*). When bound to A2, these peptides contained amino acids with potentially solvent-exposed large hydrophobic and/or aromatic side chains, which have been shown to convey immunogenicity (18, 19). Conversely, peptides 2, 8, 14, and 32 that were immunogenic only in A2 transgenic mice contained the ESO$_{110-116}$ sequence (AQDAPPL). When bound to A2, these peptides contained one or no such residue (Fig. 4, *C–E*). In accordance with this, the immunogenicity scores predicted by the IEDB immunogenicity server, which considers the TCR propensity of the peptide, were substantially lower for these than the former peptides (Table 1) (18).

However, peptide 3 contained several hydrophobic/aromatic residues, had high immunogenicity scores, yet was not immunogenic in humans and only weakly in A2 transgenic mice, arguing that immunogenicity also depends on other factors, such as: (i) in humans, but not in HLA transgenic H-$2^{-/-}$ mice, ESO peptides can be presented and recognized in the context of other HLA alleles; *e.g.* HLA-B35 and Cw3 for which immunodominant ESO CTL responses are known (27, 32, 33); (ii) the efficiency of peptide production and presentation by APC: *in silico* predictions and *in vitro* digestion experiments argue that human proteasomes produce the peptides that were immunogenic in mice, but not in humans (Fig. 4*E*) (14, 32, 66); indeed, CTLs were found in cancer patients with such specificities but other HLA restrictions (32, 33, 67); (iii) peptides binding to multiple HLA alleles, including HLA class II molecules are more immunogenic than those binding to only one allele (32, 40, 68); for the ESO$_{159-165}$ core sequence-containing peptides, there is the strongly immunogenic, DP4-restricted T-cell epitope ESO$_{157-170}$ (69), whereas for the ESO$_{110-116}$ core sequence containing peptides no $CD4^+$ T-cell epitope is known; and (iv) non-mutated TAs, including ESO, are self-antigens, and therefore TA-specific T cell responses are pruned by central tolerance in humans, which is not the case in mice that lack ESO (22, 60, 61).

In conclusion, our study demonstrated that only a small fraction of A2 binding ESO peptides was immunogenic in humans, namely those that had high peptide-binding strength and kinetic complex stability. These peptides contained multiple hydrophobic/aromatic residues, supporting the notion that immunogenicity correlates with TCR propensity. There is a need to improve *in silico* predictions of peptide-binding properties and immunogenicity of TA, namely by considering structural/conformational aspects of MHC-peptide binding, training of prediction servers with TA peptides, and refining TCR propensity calculations.

Experimental procedures

Peptides

Peptides were produced by the Protein and Peptide Chemistry Facility of the University of Lausanne, HPLC-purified (>95% pure), verified by mass spectrometry, and kept lyophilized at −80 °C.

In silico prediction of HLA-A0201 epitopes from NY-ESO-1

To predict A2 restricted ESO 8–11-mer peptides, we used the NetMHC-3.4 server (6, 42) and selected the 41 peptides scoring with an IC_{50} <3000 nM; they were additionally submitted to the NetMHC 4.0 (12) and the NetMHCpan servers (9) for binding affinity predictions and the NetMHCstab (47) and the NetMHCstabpan (16) servers for A2-ESO complex kinetic stability predictions, respectively. For immunogenicity predictions, the NetTepi server (20) and the IEDB MHC I immunogenicity servers (http://tools.iedb.org/immunogenicity/)[4] were used.

Peptide-driven refolding assay

Refolding with A2 heavy chain carrying a C-terminal BirA substrate peptide, Cy5-labeled β2m, and a test peptide were performed essentially as described (45). Human β2m was mutated Ser-88 to Cys and after refolding alkylated with maleimide-PEG_2-*Cy5* (Pierce, Thermo Fisher Scientific) in PBS at pH 7.4. Refolding reactions were performed in 96-well plates at 4 °C for 72 h in the presence of 10 μM peptide. Incubation without peptide and with the Flu $matrix_{58-66}$ peptide served as negative and positive controls, respectively. After centrifugation (4,000 rpm, 5 min), the reaction mixtures were transferred into 96-well plates, and Cy5 fluorescence was read on a fluorescence plate reader (Modulus, Promega). All measurements were performed in triplicate and data processed using Excel (Microsoft).

Peptide rebinding and pMHC complex kinetic stability assays

96-well plates were coated with streptavidin, and biotinylated A2-$MelanA_{26-35}$ complexes (1 μg/ml) were added in 50 μl and incubated for 2 h at 4 °C. The plates were saturated with biotin, washed, and incubated for 3 min at 4 °C with citrate buffer (0.13 M citric acid, 66 mM Na_2HPO_4, 150 mM NaCl, pH 4.0), followed by washing with PBS containing 0.05% Tween 20. Test peptides (10 μM) and Cy5-labeled β2m were added in PBS containing 5 mM EDTA, and the plates were incubated at 4 °C for 72 h. After washing with PBS containing 0.05% Tween 20, the A2-peptide complexes were quantified as described above. Incubations without peptide and with the Flu $matrix_{58-66}$ peptide served as negative and positive controls, respectively. The kinetic stability of complexes was assessed by incubating the A2-peptide complexes at 37 °C, and after different period of times their content was quantified likewise. The results were plotted, and half-lives were determined using GraphPad Prism software (GraphPad, San Diego, CA). All measurements were performed in triplicate.

Immunization of A2 transgenic mice

HLA-A2/DR1 transgenic, H-$2^{-/-}$ mice (38) were obtained from Taconic Models for Life, maintained in the institute's animal facility, and used in accordance with the Cantonal Veterinary Office. Groups of mice ($n = 5$) were immunized with peptides essentially as described (39). In brief, pools of five ESO peptides of similar affinities for A2 and the DR1 restricted influenza $HA_{306-318}$ peptide (10 μg each) were injected subcutaneously at the base of the tail in an emulsion containing PBS, incomplete Freund's adjuvant (IFA), and oligodinucleotides (ODN) 1826 (InvivoGen, San Diego, CA). After 2 weeks, the mice were booster-immunized, and a fortnight later their spleens were harvested, and the $CD8^+$ T cells were purified by negative selection (Stemcell Technologies, Köln, Germany) and incubated overnight with T2 cells previously pulsed with 1 μM of peptide at a 1:1 ratio. Production of IFNγ was assessed using a mouse ELISPOT kit following the manufacturer's instructions (Mabtech, Nacka Strand, Sweden).

Analysis of NY-ESO-1-specific CTLs from patient

Isolation, culturing, and stimulation of PBMC and $CD8^+$ T cells from melanoma patient NW1789 and NW3276 followed established procedures (31). In brief, purified $CD8^+$ T cells were stimulated twice with 1 μM of ESO peptides, irradiated autologous PBMC, and 150 units/ml of IL2. After a fortnight, the CTLs were tested for IFNγ production by ELISPOT following incubation with ESO peptide-pulsed T2 cells or autologous DC. A positive response was considered if the number of spots in the peptide-exposed well was >2-fold higher than the number of spots in the unstimulated well, and there were >10 specific spots/25,000 T cells. The generation of DC and the ELISPOT assay were performed as described (31).

Statistics

Statistical analyses were performed using the GraphPad Prism software (GraphPad). Correlation analyses were performed using Pearson coefficient r. The associated p value (two-tailed, $\alpha = 0.05$) quantifies the likelihood that the correlation is due to random sampling.

Author contributions—J. S. and P. G. performed the biochemical assays, which were established and optimized by D. D.; J. K. performed all the experiments on human cells; J. S. performed *in silico* predictions, data processing, and statistical analysis; I. L. and G. C. coordinated the study and edited the manuscript; and all authors discussed and interpreted the results.

Acknowledgments—We gratefully acknowledge helpful discussions with Drs. D. Gfeller, M. Bassani-Sternberg, A. Harari, R. Genolet, and D. Kouzentsov for invaluable help in data processing, presentation, and computing.

References

1. Schumacher, T. N., and Hacohen, N. (2016) Neoantigens encoded in the cancer genome. *Curr. Opin. Immunol.* **41,** 98–103
2. Schumacher, T. N., and Schreiber, R. D. (2015) Neoantigens in cancer immunotherapy. *Science* **348,** 69–74
3. Bassani-Sternberg, M., and Coukos, G. (2016) Mass spectrometry-based antigen discovery for cancer immunotherapy. *Curr. Opin. Immunol.* **41,** 9–17
4. Bassani-Sternberg, M., Bräunlein, E., Klar, R., Engleitner, T., Sinitcyn, P., Audehm, S., Straub, M., Weber, J., Slotta-Huspenina, J., Specht, K., Martignoni, M. E., Werner, A., Hein, R., Busch, H. D., Peschel, C., *et al.* (2016) Direct identification of clinically relevant neoepitopes presented on native human melanoma tissue by mass spectrometry. *Nat. Commun.* **7,** 13404
5. Lund, O., Nascimento, E. J., Maciel, M., Jr, Nielsen, M., Larsen, M. V., Lundegaard, C., Harndahl, M., Lamberth, K., Buus, S., Salmon, J., August, T. J., and Marques, E. T., Jr. (2011) Human leukocyte antigen (HLA) class

I restricted epitope discovery in yellow fewer and dengue viruses: importance of HLA binding strength. *PLoS One* **6,** e26494
6. Lundegaard, C., Lund, O., and Nielsen, M. (2008) Accurate approximation method for prediction of class I MHC affinities for peptides of length 8, 10 and 11 using prediction tools trained on 9mers. *Bioinformatics* **24,** 1397–1398
7. Vita, R., Zarebski, L., Greenbaum, J. A., Emami, H., Hoof, I., Salimi, N., Damle, R., Sette, A., and Peters, B. (2010) The immune epitope database 2.0. *Nucleic Acids Res.* **38,** D854–D862
8. Backert, L., and Kohlbacher, O. (2015) Immunoinformatics and epitope prediction in the age of genomic medicine. *Genome Med.* **7,** 119
9. Nielsen, M., and Andreatta, M. (2016) NetMHCpan-3.0: improved prediction of binding to MHC class I molecules integrating information from multiple receptor and peptide length datasets. *Genome Med.* **8,** 33
10. Carrasco Pro, S., Zimic, M., and Nielsen, M. (2014) Improved pan-specific MHC class I peptide-binding predictions using a novel representation of the MHC-binding cleft environment. *Tissue Antigens* **83,** 94–100
11. Zhang, H., Lund, O., and Nielsen, M. (2009) The PickPocket method for predicting binding specificities for receptors based on receptor pocket similarities: application to MHC-peptide binding. *Bioinformatics* **25,** 1293–1299
12. Andreatta, M., and Nielsen, M. (2016) Gapped sequence alignment using artificial neural networks: application to the MHC class I system. *Bioinformatics* **32,** 511–517
13. Trolle, T., McMurtrey, C. P., Sidney, J., Bardet, W., Osborn, S. C., Kaever, T., Sette, A., Hildebrand, W. H., Nielsen, M., and Peters, B. (2016) The length distribution of class I-restricted T cell epitopes is determined by both peptide supply and MHC allele-specific binding preference. *J. Immunol.* **196,** 1480–1487
14. Calis, J. J., Reinink, P., Keller, C., Kloetzel, P. M., and Keşmir, C. (2015) Role of peptide processing predictions in T cell epitope identification: contribution of different prediction programs. *Immunogenetics* **67,** 85–93
15. van Buuren, M. M., Calis, J. J., and Schumacher, T. N. (2014) High sensitivity of cancer exome-based CD8 T cell neo-antigen identification. *Oncoimmunology* **3,** e28836
16. Rasmussen, M., Fenoy, E., Harndahl, M., Kristensen, A. B., Nielsen, I. K., Nielsen, M., and Buus, S. (2016) Pan-specific prediction of peptide-MHC class I complex stability, a correlate of T cell immunogenicity. *J. Immunol.* **197,** 1517–1524
17. Wu, X., Xu, X., Gu, R., Wang, Z., Chen, H., Xu, K., Zhang, M., Hutton, J., and Yang, T. (2012) Prediction of HLA class I-restricted T-cell epitopes of islet autoantigen combined with binding and dissociation assays. *Autoimmunity* **45,** 176–185
18. Calis, J. J., Maybeno, M., Greenbaum, J. A., Weiskopf, D., De Silva, A. D., Sette, A., Keşmir, C., and Peters, B. (2013) Properties of MHC class I presented peptides that enhance immunogenicity. *PLoS Comput. Biol.* **9,** e1003266
19. Chowell, D., Krishna, S., Becker, P. D., Cocita, C., Shu, J., Tan, X., Greenberg, P. D., Klavinskis, L. S., Blattman, J. N., and Anderson, K. S. (2015) TCR contact residue hydrophobicity is a hallmark of immunogenic $CD8^+$ T cell epitopes. *Proc. Natl. Acad. Sci. U.S.A.* **112,** E1754–E1762
20. Trolle, T., and Nielsen, M. (2014) NetTepi: an integrated method for the prediction of T cell epitopes. *Immunogenetics.* **66,** 449–456
21. Gilchuk, P., Hill, T. M., Wilson, J. T., and Joyce, S. (2015) Discovering protective CD8 T cell epitopes: no single immunologic property predicts it!. *Curr. Opin. Immunol.* **34,** 43–51
22. Esfandiary, A., and Ghafouri-Fard, S. (2015) New York esophageal squamous cell carcinoma-1 and cancer immunotherapy. *Immunotherapy* **7,** 411–439
23. Odunsi, K., Matsuzaki, J., Karbach, J., Neumann, A., Mhawech-Fauceglia, P., Miller, A., Beck, A., Morrison, C. D., Ritter, G., Godoy, H., Lele, S., duPont, N., Edwards, R., Shrikant, P., Old, L. J., *et al.* (2012) Efficacy of vaccination with recombinant vaccinia and fowlpox vectors expressing NY-ESO-1 antigen in ovarian cancer and melanoma patients. *Proc. Natl. Acad. Sci. U.S.A.* **109,** 5797–5802
24. Valmori, D., Dutoit, V., Liénard, D., Rimoldi, D., Pittet, M. J., Champagne, P., Ellefsen, K., Sahin, U., Speiser, D., Lejeune, F., Cerottini, J. C., and Romero, P. (2000) Naturally occurring human lymphocyte antigen-A2 restricted $CD8^+$ T-cell response to the cancer testis antigen NY-ESO-1 in melanoma patients. *Cancer Res.* **60,** 4499–4506
25. Gnjatic, S., Jäger, E., Chen, W., Altorki, N. K., Matsuo, M., Lee, S. Y., Chen, Q., Nagata, Y., Atanackovic, D., Chen, Y. T., Ritter, G., Cebon, J., Knuth, A., and Old, L. J. (2002) $CD8^+$ T cell responses against a dominant cryptic HLA-A2 epitope after NY-ESO-1 peptid immunization of cancer patients. *Proc. Natl. Acad. Sci. U.S.A.* **99,** 11813–11818
26. Bioley, G., Guillaume, P., Luescher, I., Bhardwaj, N., Mears, G., Old, L., Valmori, D., and Ayyoub, M. (2009) Vaccination with a recombinant protein encoding the tumor-specific antigen NY-ESO-1 elicits an A2/157–165-specific CTL repertoire structurally distinct and of reduced tumor reactivity than that elicited by spontaneous immune responses to NY-ESO-1-expressing Tumors. *J. Immunother.* **32,** 161–168
27. Bioley, G., Guillaume, P., Luescher, I., Yeh, A., Dupont, B., Bhardwaj, N., Mears, G., Old, L. J., Valmori, D., and Ayyoub, M. (2009) HLA class I-associated immunodominance affects CTL responsiveness to an ESO recombinant protein tumor antigen vaccine. *Clin. Cancer Res.* **15,** 299–306
28. Dutoit, V., Taub, R. N., Papadopoulos, K. P., Talbot, S., Keohan, M. L., Brehm, M., Gnjatic, S., Harris, P. E., Bisikirska, B., Guillaume, P., Cerottini, J. C., Hesdorffer, C. S., Old, L. J., and Valmori, D. (2002) Multiepitope $CD8^+$ T cell response to a NY-ESO-1 peptide vaccine results in imprecise tumor targeting. *J. Clin. Invest.* **110,** 1813–1822
29. Jäger, E., Chen, Y. T., Drijfhout, J. W., Karbach, J., Ringhoffer, M., Jäger, D., Arand, M., Wada, H., Noguchi, Y., Stockert, E., Old, L. J., and Knuth, A. (1998) Simultaneous humoral and cellular immune response against cancer-testis antigen NY-ESO-1: definition of huma histocompatibility leukocyte antigen (HLA)-A2-binding peptide epitopes. *J. Exp. Med.* **187,** 265–270
30. Jäger, E., Karbach, J., Gnjatic, S., Neumann, A., Bender, A., Valmori, D., Ayyoub, M., Ritter, E., Ritter, G., Jäger, D., Panicali, D., Hoffman, E., Pan, L., Oettgen, H., Old, L. J., *et al.* (2006) Recombinant vaccinia/fowlpox NY-ESO-1 vaccines induce both humoral and cellular NY-ESO-1-specific immune responses in cancer patients. *Proc. Natl. Acad. Sci. U.S.A.* **103,** 14453–14458
31. Karbach, J., Gnjatic, S., Pauligk, C., Bender, A., Maeurer, M., Schultze, J. L., Nadler, K., Wahle, C., Knuth, A., Old, L. J., and Jäger, E. (2007) Tumor-reactive $CD8^+$ T-cell clones in patients after NY-ESO-1 peptide vaccination. *Int. J. Cancer* **121,** 2042–2048
32. Valmori, D., Lévy, F., Godefroy, E., Scotto, L., Souleimanian, N. E., Karbach, J., Tosello, V., Hesdorffer, C. S., Old, L. J., Jager, E., and Ayyoub, M. (2007) Epitope clustering in regions undergoing efficient proteasomal processing defines immunodominant CTL regions of a tumor antigen. *Clin. Immunol.* **122,** 163–172
33. Jackson, H., Dimopoulos, N., Mifsud, N. A., Tai, T. Y., Chen, Q., Svobodova, S., Browning, J., Luescher, I., Stockert, L., Old, L. J., Davis, I. D., Cebon, J., and Chen, W. (2006) Striking immunodominance hierarchy of naturally occurring $CD8^+$ and $CD4^+$ T cell responses to tumor antigen NY-ESO-1. *J. Immunol.* **176,** 5908–5917
34. Fridman, A., Finnefrock, A. C., Peruzzi, D., Pak, I., La Monica, N., Bagchi, A., Casimiro, D. R., Ciliberto, G., and Aurisicchio, L. (2012) An efficient T-cell epitope discovery strategy using in silico prediction and the iTopia assay platform. *Oncoimmunology* **1,** 1258–1270
35. Axelsson-Robertson, R., Weichold, F., Sizemore, D., Wulf, M., Skeiky, Y. A., Sadoff, J., and Maeurer, M. J. (2010) Extensive major histocompatibility complex class I binding promiscuity for Mycobacterium tuberculosis TB10.4 peptides and immune dominance of human leucocyte antigen (HLA)-B*0702 and HLA-B*0801 alleles in TB10.4 CD8 T-cell responses. *Immunology* **129,** 496–505
36. Duan, Z. L., Li, Q., Wang, Z. B., Xia, K. D., Guo, J. L., Liu, W. Q., and Wen, J. S. (2012) HLA-A*0201-restricted $CD8^+$ T-cell epitopes identified in dengue viruses. *Virol. J.* **9,** 259
37. Harndahl, M., Rasmussen, M., Roder, G., Dalgaard Pedersen, I., Sørensen, M., Nielsen, M., and Buus, S. (2012) Peptide-MHC class I stability is a better predictor than peptide affinity of CTL immunogenicity. *Eur. J. Immunol.* **42,** 1405–1416
38. Pajot, A., Michel, M. L., Fazilleau, N., Pancré, V., Auriault, C., Ojcius, D. M., Lemonnier, F. A., and Lone, Y. C. (2004) A mouse model of human

adaptive immune functions in HLA-A2.1-/HLA-DR1-transgenic H-2 class I-/class II-knockout mice. *Eur. J. Immunol.* **34,** 3060–3069
39. Boucherma, R., Kridane-Miledi, H., Bouziat, R., Rasmussen, M., Gatard, T., Langa-Vives, F., Lemercier, B., Lim, A., Bérard, M., Benmohamed, L., Buus, S., Rooke, R., and Lemonnier, F. A. (2013) HLA-A*01:03, HLA-A*24:02, HLA-B*08:01, HLA-B*27:05, HLA-B*35:01, HLA-B*44:02, and HLA-C*07:01 monochain transgenic/H-2 class I null mice: novel versatile preclinical models of human T cell responses. *J. Immunol.* **191,** 583–593
40. Nascimento, E. J., Mailliard, R. B., Khan, A. M., Sidney, J., Sette, A., Guzman, N., Paulaitis, M., de Melo, A. B., Cordeiro, M. T., Gil, L. V., Lemonnier, F., Rinaldo, C., August, J. T., and Marques, E. T., Jr. (2013) Identification of conserved and HLA promiscuous DENV3 T-cell epitopes. *PLoS Negl. Trop. Dis.* **7,** e2497
41. Lundegaard, C., Lund, O., and Nielsen, M. (2011) Prediction of epitopes using neural network based methods. *J. Immunol. Methods* **374,** 26–34
42. Lundegaard, C., Lamberth, K., Harndahl, M., Buus, S., Lund, O., and Nielsen, M. (2008) NetMHC-3.0: accurate web accessible predictions of human, mouse and monkey MHC class I affinities for peptides of length 8–11. *Nucleic Acids Res.* **36,** W509–W512
43. Trolle, T., Metushi, I. G., Greenbaum, J. A., Kim, Y., Sidney, J., Lund, O., Sette, A., Peters, B., and Nielsen, M. (2015) Automated benchmarking of peptide-MHC class I binding predictions. *Bioinformatics* **31,** 2174–2181
44. Kim, Y., Ponomarenko, J., Zhu, Z., Tamang, D., Wang, P., Greenbaum, J., Lundegaard, C., Sette, A., Lund, O., Bourne, P. E., Nielsen, M., and Peters, B. (2012) Immune epitope database analysis resource. *Nucleic Acids Res.* **40,** W525–W530
45. Guillaume, P., Legler, D. F., Boucheron, N., Doucey, M. A., Cerottini, J. C., and Luescher, I. F. (2003) Soluble major histocompatibility complex-peptide octamers with impaired CD8 binding selectively induce Fas-dependent apoptosis. *J. Biol. Chem.* **278,** 4500–4509
46. Luft, T., Rizkalla, M., Tai, T. Y., Chen, Q., MacFarlan, R. I., Davis, I. D., Maraskovsky, E., and Cebon, J. (2001) Exogenous peptides presented by transporter associated with antigen processing (TAP)-deficient and TAP-competent cells: intracellular loading and kinetics of presentation. *J. Immunol.* **167,** 2529–2537
47. Jørgensen, K. W., Rasmussen, M., Buus, S., and Nielsen, M. (2014) NetMHCstab-predicting stability of peptide-MHC-I complexes; impacts for cytotoxic T lymphocyte epitope discovery. *Immunology* **141,** 18–26
48. Salter, R. D., and Cresswell, P. (1986) Impaired assembly and transport of HLA-A and -B antigens in a mutant TxB cell hybrid. *EMBO J.* **5,** 943–949
49. Chen, J. L., Stewart-Jones, G., Bossi, G., Lissin, N. M., Wooldridge, L., Choi, E. M., Held, G., Dunbar, P. R., Esnouf, R. M., Sami, M., Boulter, J. M., Rizkallah, P., Renner, C., Sewell, A., van der Merwe, P. A., *et al.* (2005) Structural and kinetic basis for heightened immunogenicity of T cell vaccines. *J. Exp. Med.* **201,** 1243–1255
50. Ruppert, J., Sidney, J., Celis, E., Kubo, R. T., Grey, H. M., and Sette, A. (1993) Prominent role of secondary anchor residues in peptide binding to HLA-A2.1 molecules. *Cell* **74,** 929–937
51. Madden, D. R., Garboczi, D. N., and Wiley, D. C. (1993) The antigenic identity of peptide-MHC complexes: a comparison of the conformations of five viral peptides presented by HLA-A2. *Cell* **75,** 693–708
52. Thomsen, M. C., and Nielsen, M. (2012) Seq2Logo: a method for construction and visualization of amino acid binding motifs and sequence profiles including sequence weighting, pseudo counts and two-sided representation of amino acid enrichment and depletion. *Nucleic Acids Res.* **40,** W281–W287
53. Kyte, J., and Doolittle, R. F. (1982) A simple method for displaying the hydropathic character of a protein. *J. Mol. Biol.* **157,** 105–132
54. Harndahl, M., Justesen, S., Lamberth, K., Røder, G., Nielsen, M., and Buus, S. (2009) Peptide binding to HLA class I molecules: homogenous, high-throughput screening, an affinity assays. *J. Biomol. Screen.* **14,** 173–180
55. Snyder, A., and Chan, T. A. (2015) Immunogenic peptide discovery in cancer genomes. *Curr. Opin. Genet. Dev.* **30,** 7–16
56. Miles, K. M., Miles, J. J., Madura, F., Sewell, A. K., and Cole, D. K. (2011) Real time detection of peptide-MHC dissociation reveals that improvement of primary MHC-binding residues can have a minimal, or no, effect on stability. *Mol. Immunol.* **48,** 728–732
57. Wang, S., Li, J., Chen, X., Wang, L., Liu, W., and Wu, Y. (2016) Analyzing the effect of peptide-HLA-binding ability on the immunogenicity of potential $CD8^+$ and CD4+ T cell epitopes in a large dataset. *Immunol. Res.* **64,** 908–918
58. Fritsch, E. F., Rajasagi, M., Ott, P. A., Brusic, V., Hacohen, N., and Wu, C. J. (2014) HLA-binding properties of tumor neoepitopes in humans. *Cancer Immunol. Res.* **2,** 522–529
59. McMahan, R. H., McWilliams, J. A., Jordan, K. R., Dow, S. W., Wilson, D. B., and Slansky, J. E. (2006) Relating TCR-peptide-MHC affinity to immunogenicity for the design of tumor vaccines. *J. Clin. Invest.* **116,** 2543–2551
60. Anderson, M. S., and Su, M. A. (2016) AIRE expands: new roles in immune tolerance and beyond. *Nat. Rev. Immunol.* **16,** 247–258
61. Khan, I. S., Mouchess, M. L., Zhu, M. L., Conley, B., Fasano, K. J., Hou, Y., Fong, L., Su, M. A., and Anderson, M. S. (2014) Enhancement of an anti-tumor immune response by transient blockade of central T cell tolerance. *J. Exp. Med.* **211,** 761–768
62. Duan, F., Duitama, J., Al Seesi, S., Ayres, C. M., Corcelli, S. A., Pawashe, A. P., Blanchard, T., McMahon, D., Sidney, J., Sette, A., Baker, B. M., Mandoiu, I. I., and Srivastava, P. K. (2014) Genomic and bioinformatic profiling of mutational neoepitopes reveals new rules to predict anticancer immunogenicity. *J. Exp. Med.* **211,** 2231–2248
63. Hawse, W. F., Gloor, B. E., Ayres, C. M., Kho, K., Nuter, E., and Baker, B. M. (2013) Peptide modulation of class I major histocompatibility complex protein molecular flexibility and the implications for immune recognition. *J. Biol. Chem.* **288,** 24372–24381
64. Madura, F., Rizkallah, P. J., Holland, C. J., Fuller, A., Bulek, A., Godkin, A. J., Schauenburg, A. J., Cole, D. K., and Sewell, A. K. (2015) Structural basis for ineffective T-cell responses to MHC anchor residue-improved "heteroclitic" peptides. *Eur. J. Immunol.* **45,** 584–591
65. Insaidoo, F. K., Borbulevych, O. Y., Hossain, M., Santhanagopolan, S. M., Baxter, T. K., and Baker, B. M. (2011) Loss of T cell antigen recognition arising from changes in peptide and major histocompatibility complex protein flexibility: implications for vaccine design. *J. Biol. Chem.* **286,** 40163–40173
66. Nielsen, M., Lundegaard, C., Lund, O., and Keşmir, C. (2005) The role of the proteasome in generating cytotoxic T-cell epitopes: insights obtained from improved prediction of proteasomal cleavage. *Immunogenetics* **57,** 33–41
67. Chen, J. L., Dawoodji, A., Tarlton, A., Gnjatic, S., Tajar, A., Karydis, I., Browning, J., Pratap, S., Verfaille, C., Venhaus, R. R., Pan, L., Altman, D. G., Cebon, J. S., Old, L. L., Nathan, P., *et al.* (2015) NY-ESO-1 specific antibody and cellular responses in melanoma patients primed with NY-ESO-1 protein in ISCOMATRIX an boosted with recombinant NY-ESO-1 fowlpox virus. *Int. J. Cancer* **136,** E590–E601
68. de Melo, A. B., Nascimento, E. J., Braga-Neto, U., Dhalia, R., Silva, A. M., Oelke, M., Schneck, J. P., Sidney, J., Sette, A., Montenegro, S. M., and Marques, E. T. (2013) T-cell memory responses elicited by yellow fever vaccine are targeted to overlapping epitopes containing multiple HLA-I and -II binding motifs. *PLoS Negl. Trop. Dis.* **7,** e1938
69. Zeng, G., Wang, X., Robbins, P. F., Rosenberg, S. A., and Wang, R. F. (2001) $CD4^+$ T cell recognition of MHC class II-restricted epitopes from NY-ESO-1 presented by a prevalent HLADP4 allele: association with NY-ESO-1 antibody production. *Proc. Natl. Acad. Sci. U.S.A.* **98,** 3964–3969
70. Hopp, T. P., and Woods, K. R. (1981) Prediction of protein antigenic determinants from amino acid sequences. *Proc. Natl. Acad. Sci. U.S.A.* **78,** 3824–3828
71. Abraham, D. J., and Leo, A. J. (1987) Extension of the fragment method to calculate amino acid zwitterion and side chain partition coefficients. *Proteins* **2,** 130–152
72. Black, S. D., and Mould, D. R. (1991) Development of hydrophobicity parameters to analyze proteins which bear post- or cotranslational modifications. *Anal. Biochem.* **198,** 72–82
73. Sweet, R. M., and Eisenberg, D. (1983) Correlation of sequence hydrophobicities measures similarity in three-dimensional protein structure. *J. Mol. Biol.* **171,** 479–488
74. Roseman, M. A. (1988) Hydrophobicity of the peptide C=O . . . H-N hydrogen-bonded group. *J. Mol. Biol.* **201,** 621–623